INTERNATIONAL JOURNAL OF PRECISION ENGINEERING AND MANUFACTURING Vol. 19, No. 1, pp. 67-78 JANUARY 2018 / 67

REGULAR PAPER

DOI: 10.1007/s12541-018-0008-0
ISSN 2234-7593 (Print) / 2005-4602 (Online)

Some Insights on Combined Turning-Burnishing (CoTuB) Process on Workpiece Surface Integrity

Anis Rami[1,2], Fathi Gharbi[2,#], Salem Sghaier[2], and Hedi Hamdi[1]

1 Department of Mechanical Engineering, Université de Lyon, ENISE, CNRS UMR 5513, LTDS, F-42023, Saint-Etienne, France
2 Department of Mechanical Engineering, Université de Monastir, ENIM, LGM, Avenue Ibn Eljazzar, 5000. Monastir, Tunisia
Corresponding Author / E-mail: fathi.gharbi@yahoo.fr, TEL: +216-52-844-960

KEYWORDS: Turning, Burnishing, Surface integrity, Experimentation

This paper deals with a combined manufacturing process called Combined Turning-Burnishing (CoTuB) that performs turning and ball-burnishing simultaneously on the same machine tool. This innovative process aimed to enhance surface quality and integrity by exploiting rough turning conditions. Consequently, this implies an increase in productivity when compared to conventional surface treatment processes. For this reason, a device was manufactured in order to hold both commercial cutting and burnishing tools to carry out the removal material and the surface mechanical treatment processes simultaneously and under the same operation. As the design of CoTuB device sets the cutting tool ahead of the ball, turning is followed by burnishing operation along the manufactured surface. It has been depicted experimentally that a considerable improvement in surface quality could be achieved using the new combined process under suitable process parameters. Burnishing force, Ball burnishing diameter and depth of cut are independent parameters. In order to carry out a parametric process study, several experiments based on Taguchi method were performed. The aim is to identify the optimal turning/burnishing parameters when treating AISI 4140 steel. This helps to get a compromise between the optimal arithmetic surface roughness (Ra), the compressive residual stress state and the micro-hardness (μH).

Manuscript received: April 12, 2017 / Revised: June 26, 2017 / Accepted: July 6, 2017

NOMENCLATURE

CoTuB = Combined Turning /Burnishing process
V_C = Cutting speed (m/min)
f = Feed rate (mm/rev)
a_p = Depth of cut (mm)
F_B = Burnishing force (N)
ϕ_B = Ball burnishing diameter (mm)
R_a = Arithmetic mean roughness (μm)
μH = micro-hardness (HV)
HV = Vickers micro-hardness scale (HV)
HRC = Rockwell micro-hardness scale (HRC)
RS = Residual Stress
X_i = Regression Coefficient
DoF = Degrees of Freedom
A, B, C, D and E = Variables representing different CoTuB Parameters and it interactions
OA = Orthogonal Arrays
F_i = Factors of design of experiments
T = Trial Numbers
n_i = Number of levels
K = Constant of Taguchi Design
SCM = Smallest Common Multiple
σ_{yy} = Residual stress in the feed direction (MPa)
σ_{xx} = Residual stress in the burnishing direction (MPa)
r_ε = Tool noise radius (mm)
K_r = Approach angle (°)
α = Clearance angle (°)
γ = Rake angle (°)
λ = Cutting edge inclination angle (°)

1. Introduction

The surface integrity is generally defined and specified in terms of

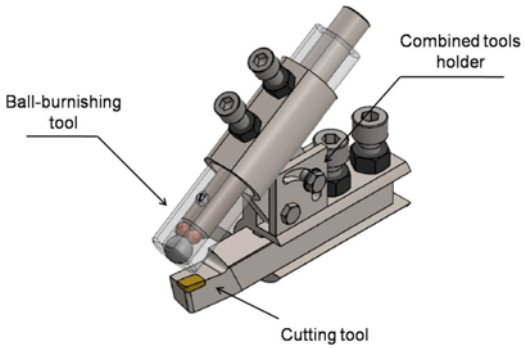

Fig. 1 Schematic representation of the manufactured CoTuB device exploited in the present research work

surface topography, state of residual stress, and microstructure. Mainly, low value of roughness, high compressive residual stress, and high micro-hardness in the superficial layer, leading to an improvement in the component's corrosion, wear and fatigue resistances.[1-5] However, the application of a machining process (turning, milling) as finishing treatment is inefficient due to the generation of a low surface quality especially characterized by tensile residual stresses produced in the external surface. To overcome this limitation, several treatments were deployed for the major aim to improve surface quality, i.e. providing a good surface roughness and converting tensile residual stresses to compressive ones and hardening surface.

The treatment operations can be classified according to their physical impact on the machined surface such as thermal (quenching, tempering, etc.), Mechanical (shot peening, rolling, burnishing, etc.) and chemical (carburizing, nitriding, etc.). As a matter of fact, the ball burnishing process is one of the most widespread treatments providing a good surface integrity and a less cost compared to other processes.[6] Burnishing is a cold working surface treatment process without material removal. During this process, plastic deformation of surface irregularities occurs by applying pressure through a very hard and smoothed ball surface. As a result, all pre-machined peaks are compressed thus giving a finished surface. However, the conventional operation, through the hardening impact, is limited at the external surface while the objective is to reach a greater hardened depth of the workpiece. The abundant heat provided along cutting operation contributes to soften the superficial layer of the workpiece. Mainly, due to the low heat transfer coefficient of AISI 4140 steel, the generated heat in workpiece surface softens it. Thus, an elastic deformation on the workpiece surface is involved.[7] Consequently, burnishing, synchronized with cutting, added to the softening and elastic deformation around cutting regions increase the hardening depth. This technique is inspired from some hybrid processes used in manufacturing such as laser-assisted and ultrasonically-assisted machining which are designed to enhance the workpiece surface quality.

Fig. 1 illustrates the manufactured CoTuB device used in the present research work. It allows to combine both cutting and burnishing processes in the purpose to enhance the generated surface proprieties and beneath the surface cooperatively with saving time and cost compared to conventional processes. However, in order to realize a successful performance with a good surface integrity, the effect of parameters governing the process must be studied. The cutting process parameters are the cutting speed (V_C), depth of cut (a_P) and feed rate (f). The parameters of ball burnishing process are mainly burnishing speed (V_B), burnishing force (F_B), ball diameters (ϕ_B) and burnishing feed rate (f_B). In this current case, the mechanical treatment and the cutting operation were concurrently performed by means of the new CoTuB device. Some parameters corresponding to cutting and ball burnishing processes become dependent such as cutting speed and burnishing speed, cutting feed rate and burnishing feed rate. Therefore, it is quite necessary to investigate the effects of CoTuB parameters on the generated surface.

2. Literature Review

2.1 Similar combined process

The combined machining-burnishing process and its effects on the surface integrity have been documented in other works. Mezlini el al.[8] showed that using the combined machining/burnishing tool reduces the manufacturing cost by up to 4 times. Also, they showed that a surface arithmetic roughness (R_a) is reduced by 58% compared to classic turning finishing process. A maximum of compressive residual stresses is reached in the layer surface, and the layer's micro-hardness is increased. In other work, Shirsat and Ahuja[9] showed that combining turning and burnishing, improve final surface arithmetic roughness (R_a) from 0.75 μm down to 0.11 μm. They also confirm that the variation of the applied burnishing force has a significant effect on the surface hardness evolution. Axinte and Gindy[10] showed that using Turning Assisted with Deep Cold Rolling tool, surface roughness become smooth with a mirror polished appearance and metallurgical analysis revealed a significant work-hardening effect up to 300 μm beneath the surface.

2.2 Effect of cutting parameters on surface integrity

Many studies in the literature focused on optimizing the different parameters governing turning and/or burnishing processes but separately. Indeed, it is known that the main governing parameters of cutting process, among others, are essentially, cutting speed feed rate and cutting depth. The latter, can affect the properties of superficial layers and the quality of surface finishing.[11] For example, several studies have demonstrated that cutting speed and feed rate influence roughness evolution. Aouici et al.[12] have shown that an improved surface roughness can be achieved at lower feed rate and higher cutting speed. Other research works focused on the effect of cutting conditions on the distribution of residual stresses after machining.[13,14] By increasing the cutting speed, residual stresses have tendency to promote tensile stress state as it was presented in[13] whereas a low cutting speed decreases the magnitude of these stresses. The tool wear may also affect residual stresses evolution as it was demonstrated in[14,15] where it was shown that a worn tool edge causes tensile residual stresses than a new one. Moreover, it is known that, machining operations can yield to a plastically layer implying a rise in surface hardness.[16] The thickness of the affected plastic layer increases with cutting speed and feed rate variations.

Table 1 Chemical composition of workpiece (AISI 4140) and ball material (AISI 52100)

Composition (%)	C	Si	Mn	P	S	Cr	Mo
AISI 4140	0.41	0.39	0.72	0.025	0.035	1.12	0.27
AISI 52100	1.02	0.25	0.34	0.025	0.015	1.50	0.10

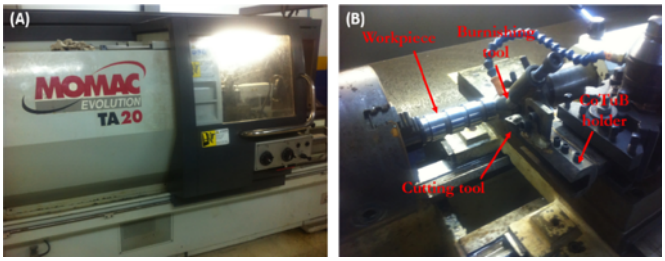

Fig. 2 Combined devices mounted on NC lathe

2.3 Effect of burnishing parameters on surface integrity

For burnishing process, it has been concluded that the burnishing force and the ball diameter are the major parameters affecting the plastic deformation level in the surface layer.[3,17-20] A high burnishing force decreases surface roughness, increases hardness[21-24] and also generates a compressive residual stress. All these provide the increase of surface resistances regarding fatigue,[16,24-26] wear,[27,28] and corrosion.[29] The tool pass number of burnishing can also improve the surface properties.[28]

2.4 CoTuB process

The main contribution of the presented experimental work is to predict and to optimize surface roughness (R_a), residual stresses and micro-hardness of AISI 4140 steel based on CoTuB process. In order such objective, a new experimental set-up that combines turning operation with a ball-burnishing tool was designed, manufactured and produced. This helps to crash the micro-geometric irregularities generated during cutting under the action of the ball-burnishing tool. The idea is to take into account the benefits of cutting temperature during the pass and to increase the magnitude of plastic deformation located on the cut surface. Along the CoTuB process, three types of parameters are involved namely: (i) turning parameters (V_c, a_p and f), (ii) burnishing ones (ϕ_B and F_B) and (iii) common parameters (V_c and f). In all what follow, the Taguchi technique will be implemented to investigate the effect of CoTuB process parameters on the surface integrity. Moreover, it is important to spotlight that CoTuB process offers a number of potential advantages beside the classic surface treatment ones, thanks to lower costs of equipment and the higher productivity rate.

3. Experimental Methodology

3.1 Workpiece material and experimental procedure

As mentioned earlier, a combined turning/burnishing (CoTuB) device was designed and manufactured in order to simultaneously accomplish both turning and burnishing operations on AISI 4140 steel. The materials chemical composition in wt% and mechanical behaviors, of the ball (AISI 52100) are detailed in Table 1. Experimental tests

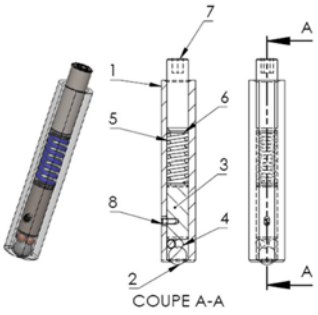

N°	Nomenclature	QTY
8	Position bolt	1
7	Pressure bolt	1
6	Washer	2
5	Calibrating spring	1
4	Support ball	3
3	Cleat wear	1
2	Ball burnishing	1
1	Tool body	1

Fig. 3 Ball burnishing tool assembly

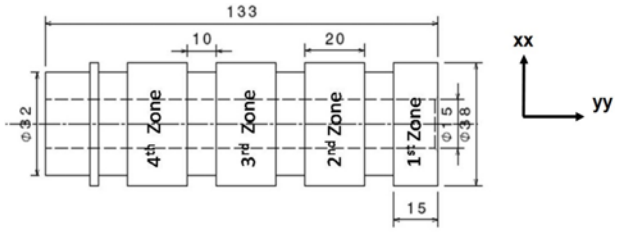

Fig. 4 AISI 4140 workpiece prepared for combined turning-ball burnishing

were carried out on NC lathe, Model: MOMAC Evolution TA 20 with a Fanuc Post processor (Fig. 2). The CoTuB device corresponds to the use of cutting tool and ball-burnishing one. The idea is to obtain at the same time a finished surface by turning and burnishing operations. The holder presented in Fig. 2(B) has the advantage to maintain both the cutting and the ball burnishing tools. Cutting and burnishing tools are rigidly held in the holder that is easily fitted on the turret of the lathe used.

The cutting tool used is a carbide insert, of a standard designation CNMG 12 04 12 PR 4225, and mounted on PCLNR 2020KL112 CANELA tool holder. Its geometry is characterized by a tool noise radius: r_ε = 0.8 mm and the following angles: approach angle K_r = 75°, clearance angle α = 6°, rake angle γ = 6° and cutting edge inclination angle λ = 0°. As shown in Fig. 3, the ball burnishing tool has a ball with an arithmetic surface roughness R_a = 0.03 μm and hardness equals to 63 HRC.

3.2 Workpiece preparation

Specimen were extracted from an AISI 4140 cylindrical bar and prepared according to the drawing of Fig. 4. Workpiece is initially turned to 38 mm diameter with carbide cutting tool (PCLN) on NC lathe with a spindle speed of 800 rpm and a feed rate of 0.2 mm/rev. The initial surface roughness R_a was measured.

In the second step, specimen is turned to have 4 zones separated by grooves (Fig. 4). In actual design of experiments, by applying different parameters on each zone, this long workpiece can be used as 3 different workpieces. The zone 1 serves to calibrate the burnishing force for a fixed depth of cut. The 2nd, 3rd and 4th zones were used to make experimental tests, where in a set of feed rate are assigned 0.15, 0.1, 0.05 mm/rev, respectively. The experiments were carried out on 9 workpieces (Fig. 5) implying the realization of 27 tests.

Fig. 5 Surface roughness measurements

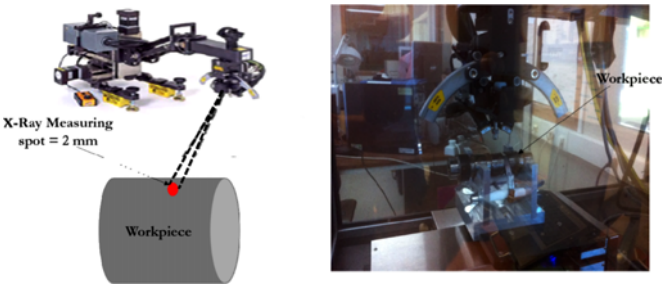

Fig. 6 Spot size of the X-Ray machine and X-Ray diffraction

3.3 Experimental characterizations and measurements

After the CoTuB operation, values of arithmetic mean roughness (R_a) were measured by using the MITUTOYO surf test SJ-210 with a cut-off length of 0.8 mm and a sampling length of 4 mm. As depicted in Fig. 6, two components of residual stress, feed direction σ_{yy} and burnishing direction σ_{xx}, were recorded using a MGR40 X-Ray diffraction head and equipped with a 2 mm diameter collimator provided by PROTO Company. The measurement conditions are listed below:

- Diffraction conditions:
  - Cr Kα radiation with 18 kV, 4 mA.
  - λ = 0.229 nm, planes {211}.
  - Bragg's angles: $2\theta = 156^{o}$.
  - Ω acquisition mode.
- Acquisition conditions:
  - 7 β-angles (from -30° to +30°) in both directions X and Y.
  - β oscillations: ±6°.
- Stress calculation:
  - Elliptic treatment method.
  - Radio crystallographic elasticity constants:

$1/2\ S_2 = 5.92 \times 10^{-6}\ \text{MPa}^{-1}$

$S_1 = -1.28 \times 10^{-6}\ \text{MPa}^{-1}$

An in-depth investigation of residual stress distribution following a successive layer removal has been carried out using an electrochemical polishing system (Fig. 7). Micro-hardness was measured by a Wilson Hardness Tester Model 402 MVD, (ITW Test & Measurement, (Shanghai) Co. Ltd) with a Vickers indenter under 500g load. The micro-hardness values were determined on the external surface and beneath the turned/burnished surface as illustrated in Fig. 8. Finally, a Scanning Electron Microscope was used to visualize the micro-structures changes.

Fig. 7 Electro-polishing machine

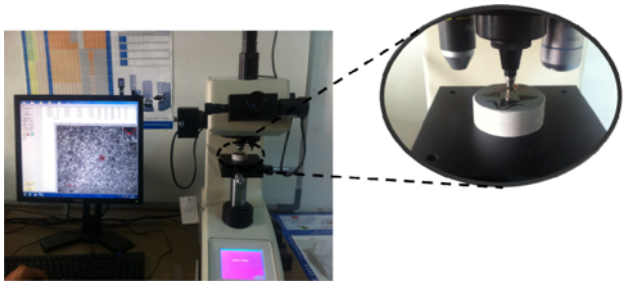

Fig. 8 Micro-hardness measuring

Table 2 Assignment of the levels to factors

Factors	Levels		
	1	2	3
Ball Diameter Φ_B (mm)	08	10	12
Burnishing force F_B (N)	100	150	200
Cutting speed V_C (m/min)	100	125	150
Depth of cut a_p (mm)	0.5	0.75	1
Feed rate f (mm/rev)	0.05	0.1	0.15

3.4 Taguchi method for design of experiments

It is important to underline that the main objective of the present study is to highlight the influence of the combined parameters governing the CoTuB process and their optimum level combinations on surface integrity. To evaluate which parameters of the CoTuB process affect the distributions of surface roughness, residual stresses, and surface hardness, the Taguchi method was used at various steps to carry out the tests. These steps are detailed below.

3.4.1 Identification of experiment outputs

Surface roughness (R_a) of the workpiece, residual stresses both in the feed and the burnishing directions, named σ_{yy} and σ_{xx}, respectively, are the important outputs having an impact on the workpiece's lifetime and the micro-hardness (μH). The latter affects considerably the wear resistance of superficial layer.

3.4.2 Selection of the factors and their levels

The operating conditions such as ball diameter, burnishing force, cutting speed, depth of cut and feed rate were considered as controllable parameters during this experimental work. Three levels were selected for each factor with equal spacing as shown in Table 2. The range of turning parameters was selected from a Sandvik catalog,

Table 3 Measured quality outputs for CoTuB process based on Taguchi design of experiments (standard L27)

Trial N	CoTuB Parameters					Results			
						Roughness	Residual stresses		μHardness
	Ball Diameter (mm)	Burnishing Force (N)	Cutting Speed (m/min)	Depth of Cut (mm)	Feed Rate (mm/rev)	Ra (μm)	σ_{yy} (MPa)	σ_{xx} (MPa)	μH (HV)
1	12	200	150	1.50	0.15	0.446	-500.28	-216.75	278
2	12	200	150	1.50	0.10	0.725	-588.13	-239.09	264
3	12	200	150	1.50	0.05	0.383	-771.21	-327.94	278
4	12	150	125	1.00	0.15	0.924	-430.28	-38.02	231
5	12	150	125	1.00	0.10	0.593	-540.83	-200.27	318
6	12	150	125	1.00	0.05	0.263	-485.73	-265.43	320
7	12	100	100	0.50	0.15	0.821	-574,98	-176.32	208
8	12	100	100	0.50	0.10	0.400	-551.75	-244.35	231
9	12	100	100	0.50	0.05	0.189	-637.63	-321.63	215
10	10	200	125	0.50	0.15	0.813	-520.13	-192.92	286
11	10	200	125	0.50	0.10	0.521	-415.27	-234.71	262
12	10	200	125	0.50	0.05	0.726	-630.14	-254.22	252
13	10	150	100	1.50	0.15	0.263	-606.4	-286.95	252
14	10	150	100	1.50	0.10	1.822	-271.98	-154.95	362
15	10	150	100	1.50	0.05	2.281	-206,74	-72.37	265
16	10	100	150	1.00	0.15	0.484	-683.08	-251.15	342
17	10	100	150	1.00	0.10	0.376	-744.26	-380.87	253
18	10	100	150	1.00	0.05	0.360	-741.11	-388.19	265
19	08	200	100	1.00	0.15	0.555	-891.05	-427.70	397
20	08	200	100	1.00	0.10	1.083	-1005.23	-395.12	382
21	08	200	100	1.00	0.05	0.439	-698.83	-441.64	320
22	08	150	150	0.50	0.15	0.690	-820.40	-346.71	374
23	08	150	150	0.50	0.10	1.005	-723.12	-302.04	372
24	08	150	150	0.50	0.05	0.955	-890.24	-342.15	423
25	08	100	125	1.50	0.15	0.688	-524.57	-78.53	343
26	08	100	125	1.50	0.10	0.558	-535.76	-145.55	347
27	08	100	125	1.50	0.05	0.279	-518.08	-130.15	347

and the range of burnishing parameters was made from previous experimental work investigation.[3,8,9]

3.4.3 Selection of the Taguchi Orthogonal Arrays

Taguchi Orthogonal Arrays (*OA*) is selected based on the *DoF* (Degree of Freedom) of the experimental design. The aim of selecting the Taguchi *OA* is to identify before conducting the experiment which interactions might be more significant. In the case of our experiment, the total *DoF* is established as follows:

Without interaction

$$DoF = (n_1-1)F_1+(n_2-1)F_2+(n_3-1)F_3+(n_4-1)F_4+(n_5-1)F_5$$
$$DoF = 2\times 5 = 10 \quad (1)$$

Where: n_i the number of levels, and F_i the factors.

With interaction (Significant interactions)

$$DoF = 10+(n_1-1)(n_2-1)F_1F_2+(n_1-1)(n_3-1)F_1F_3 + (n_1-1)(n_4-1)F_1F_4+(n_1-1)(n_5-1)F_1F_5 \quad (2)$$
$$DoF = 10+(3-1)(3-1)\times 4 = 10+16 = 26$$

Taguchi's condition

$$T \geq DoF = 26$$
$$T = k\times SCM\,;\ k = (1,2,\ldots,n) \Rightarrow T = 1\times((3\times 3)\times 3) = 27\ Tests \quad (3)$$

Where: *T*: the numbers of trials, *SCM*: Smallest Common Multiple.

The Taguchi *OA* chosen is L27, which has 27 rows corresponding to the Taguchi's conditions calculated above (26 *DoF*) as shown in table 3. For each combination resulting in total of 27 runs, only one test was established.

Therefore, to complete the statistical analysis of the experiments, four quality outputs were measured, i.e. surface roughness R_a, residual stresses in the feed direction σ_{yy}, residual stresses in the burnishing direction σ_{xx}, and the micro-hardness μH (Table 3).

3.5 Determination of the interaction and regression model

A polynomial regression model was established as indicated in Eq. 4. The equation is based on mathematical and analysis predicting responses. MINITAB16 software was used. The interaction terms in the proposed regression model affecting results were statistically determined through the Pareto's diagram as shown in Fig 9. In this case, the regression model can be expressed as follows:

$$Y = X_0+X_1(A)+X_2(B)+X_3(C)+X_4(D)+X_5(E) + X_6(AC)+X_7(AE)+X_8(BD)+X_9(CD) \quad (4)$$

Where: *Y*: process output quality, X_0: constant; *A*, *B*, *C*, *D*, *E* are variables representing different CoTuB parameters; and the X_i are the regression coefficients and interactions.

Table 4 Experimental design and results of signal-to-noise (S/N) ratio for the different outputs

Trial N	Ra (μm)	σ_{yy} (MPa)	σ_{xx} (MPa)	μH (HV)	S/N Ratio for Ra	S/N Ratio for σ_{yy}	S/N ratio for σ_{xx}	S/N Ratio for μH
1	0.446	-500.28	-216.75	278	7.0133	53.9843	46.7192	48,8809
2	0.725	-588.13	-239.09	264	2.7932	55.3895	47.5712	48,4321
3	0.383	-771.21	-327.94	278	8.3360	57.7435	50.3159	48,8809
4	0.924	-430.28	-38.02	231	0.6866	52.6750	31.6002	47,2722
5	0.593	-540.83	-200.27	318	4.5389	54.6612	46.0323	50,0485
6	0.263	-485.73	-265.43	320	11.6009	53.7279	48.4790	50,1030
7	0.821	-574.98	-176.32	208	1.7131	55.1931	44.9260	46,3613
8	0.400	-551.75	-244.35	231	7.9588	54.8348	47.7602	47,2722
9*	0.189	-637.63	-321.63	215	14.4708	56.0914	50.147	46,6488
10	0.813	-520.13	-192.92	286	1.7982	54.3222	45.7075	49,1273
11	0.521	-415.27	-234.71	262	5.6632	52.3666	47.4106	48,3660
12	0.726	-630.14	-254.22	252	2.7813	55.9887	48.1042	48,0280
13	0.263	-606.40	-286.95	252	11.6009	55.6552	49.1561	48,0280
14	1.822	-271.98	-154.95	362	-5.2110	48.6907	43.8038	51,1742
15	2.281	-206.74	-72.37	265	-7.1625	46.3085	37.1912	48,4649
16	0.484	-683.08	-251.15	342	6.3031	56.6894	47.9987	50,6805
17	0.376	-744.26	-380.87	253	8.4962	57.4345	51.6155	48,0624
18*	0.360	-741.11	-388.19	265	8.8739	57.3977	51.780	48,4649
19	0.555	-891.05	-427.70	397	5.1141	58.9980	52.6228	51,9758
20	1.083	-1005.23	-395.12	382	-0.6926	60.0453	51.9346	51,6413
21*	0.439	-698.83	-441.64	320	7.1507	56.8874	52.9014	50,1030
22	0.690	-820.40	-346.71	374	3.2230	58.2805	50.7993	51,4574
23	1.005	-723.12	-302.04	372	-0.0433	57.1842	49.6013	51,4109
24	0.955	-890.24	-342.15	423	0.3999	58.9901	50.6843	52,5268
25	0.688	-524.57	-78.53	343	3.2482	54.3961	37.9007	50,7059
26	0.558	-535.76	-145.55	347	5.0673	54.5794	43.2602	50,8066
27	0.279	-518.08	-130.15	347	11.0879	54.2879	42.2889	50,8066

*: Trial corresponding to the optimal CoTuB parameters

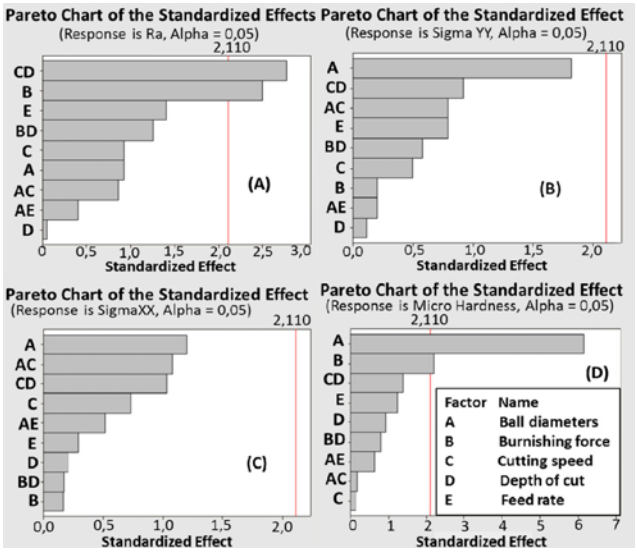

Fig. 9 Pareto's Diagram for standardized effect of quality characteristics

4. Results and discussion

4.1 Evaluation of S/N ratios

Table 4 shows the experimental results and calculated S/N ratios for every output. As indicated, the surface roughness is measured in range of [0.189 μm; -2,281 μm], feed and burnishing residual stresses are in range of [-38.02 MPa; -441.64 MPa] and [-206.74 MPa; -1005.23 MPa], respectively, and micro-hardness is in a range of [458 HV; 673 HV].

From Table 3, the optimal outputs in terms of mean arithmetic roughness, compressive stresses and micro-hardness are chosen for each ball burnishing diameter (12, 10 and 8 mm).

These outputs, which are considered as optimal ones, are selected based on the S/N ratio evaluation presented in Table 4 in relationship with Trials N 9, 18 and 21, respectively. The aim of this selection is to compare CoTuB outputs and the turned surface ones.

The chosen trial offers the best satisfaction compromise for the response quality, such as surface roughness, residual stress for feed and burnishing directions reaching the maximum compression peak beneath all trials, as well the maximum micro-hardness value.

4.2 Surface quality responses

4.2.1 Effects of controllable parameters on surface roughness evolution

Fig. 10 shows that optimal surface roughness is revealed at low feed rate i.e. 0.05 mm/rev, thanks to the small distance between the successive traces of the cutting tool and the ball burnishing one along the workpiece during CoTuB process. In this case, the ball has the advantage to flatten out the bulge edges of the former traces caused by

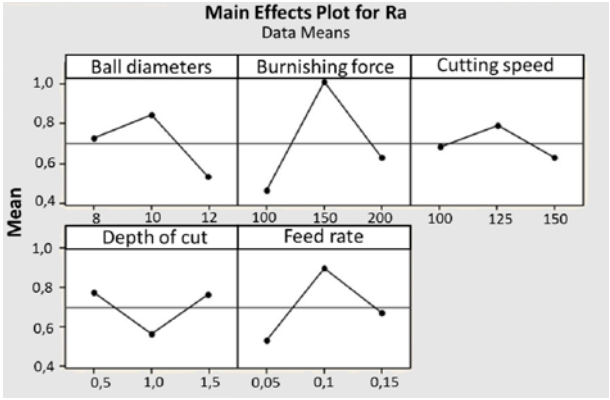

Fig. 10 Main effects plot of surface roughness versus controllable parameters

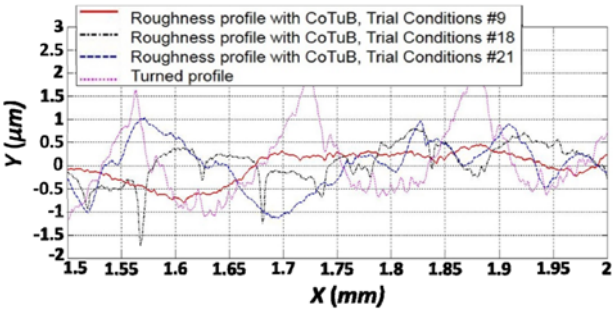

Fig. 11 Surface arithmetic roughness, Ra, according to ball diameter variation and compared to turning operation

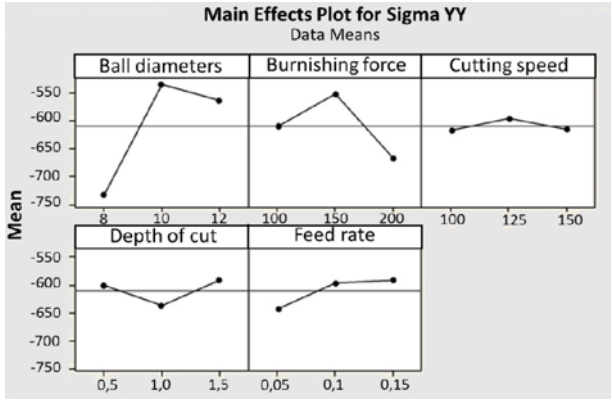

Fig. 12 Main effect plot of residual stresses in the feed direction versus controllable parameters

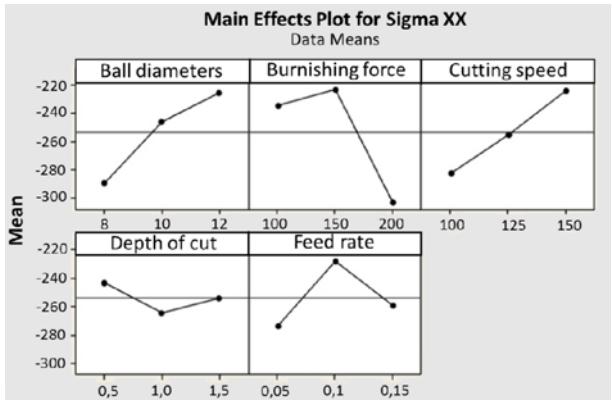

Fig. 13 Main effects plot of residual stresses in the burnishing direction versus controllable parameters

the cutting edge.

This enhancement of surface roughness is promoted when a larger ball burnishing diameter was used i.e. 12 mm. Indeed, the lower the ball diameter, the higher the distance between two succeeding indentations. This induces an increasing of surface roughness. It must be highlighted also that surface roughness decreases appreciably in case of low value of burnishing force i.e. 100 N. This performance is due to the fact that the ball burnishing penetrated along small distance into the work surface. Consequently, it causes a little deformation of the asperities. The surface roughness increases for a high range of force 150-200 N. This can be explained by the ploughing of metal appearing on ball trajectory side.

Also shown in Fig. 10 is the minimum value of surface roughness that was reached when the depth of cut was about 1 mm. A lower depth of cut was adopted i.e. 0.5 mm allowing to have a small chip fragments inserted between the ball and the work surface during the CoTuB operation, inducing a scratched surface. It should be noted here that the cutting speed has no significant effect on the value of surface roughness.

In addition as illustrated in Fig. 10, a low feeds rate and low burnishing force with a larger ball burnishing diameters are advantageous to obtain an optimal surface roughness. From trials N 9, 18 and 21, it appears that the final surface roughness quality (R_a) obtained is close to the roughness values of grinding process, reaching 0.189 µm.

Fig. 11 shows the 2D profile of the surface topography corresponding to the surface generated by CoTuB and turning processes. As shown, a decrease of the arithmetic mean roughness (R_a) is achieved in the case of the CoTuB process for different ball-burnishing diameters (8, 10 and 12 mm). Indeed, irregularity peaks are considerably erased against valleys yielding to a lower roughness in comparison with the one generated by turning operation, which is equal to 0.81 µm in the present case.

The generated cutting temperature along with the normal force applied through the ball burnishing during the CoTuB process induces a plastic deformation in the new surface. This indicated a decreasing of the highest of strips generated by cutting insert during turning process. Here, the effect of ball-burnishing diameter size is also underlined. This is the parameter that highly governs the arithmetic roughness evolution because it leads to a flattening of the peaks into valley especially for lower feed rate. It is important to note that larger ball diameters yielded an improvement in the surface roughness. The modification of the roughness profile obtained with a ball diameter of 12 mm (R_a = 0.189 µm) as compared to the ball diameter of 10 mm (R_a = 0.36 µm) and 8mm (R_a = 0.439 µm). These results are obtained despite the magnitude of the force applied by the ball in case of 8mm, which is twice higher than that applied in the other cases. Generally, the surface roughness is obviously improved when using the CoTuB process compared to the classically turned surface (R_a = 0.81 µm). As a matter of fact, roughness surface increases up to 70% using the CoTuB process.

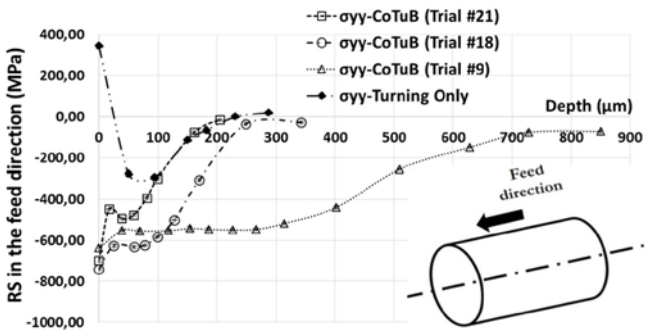

Fig. 14 Residual stresses evolution along the feed direction versus depth

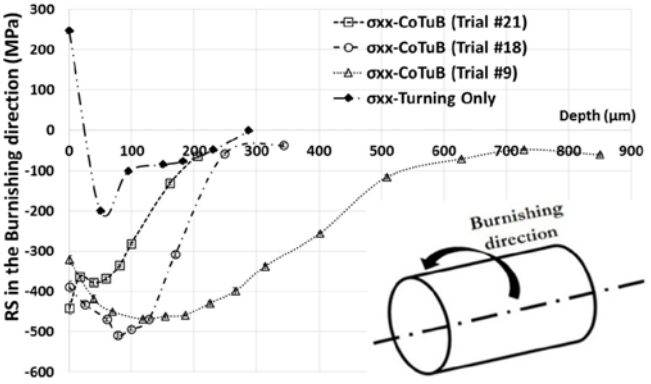

Fig. 15 Residual stresses evolution along the burnishing direction versus the depth

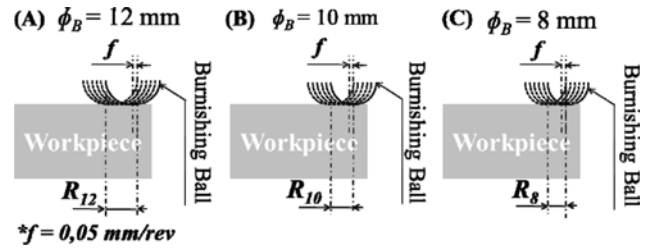

Fig. 16 Schematic representation of the recovery rate for different ball diameters; (A) ϕ_B = 12 mm, (B) ϕ_B = 10 mm and (C) ϕ_B = 8 mm

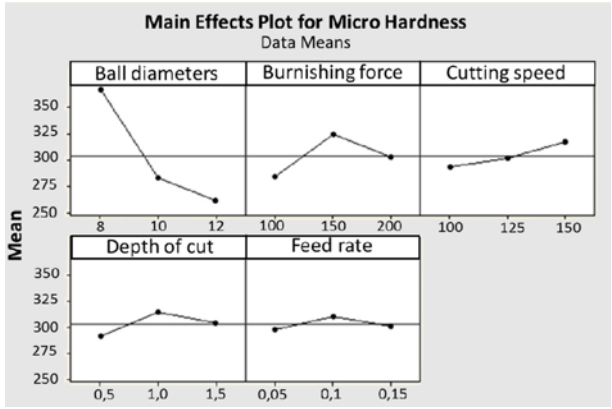

Fig. 17 Main effects plot of micro-Hardness versus controllable parameters

4.2.2 Effects of controllable parameters on residual stress evolution

As indicated in Figs. 12 and 13, the ball burnishing diameter and the burnishing force have major influence on the residual stresses both in feed and burnishing directions. The maximum value of compressive residual stress was obtained with the lower diameter of ball burnishing i.e. 8 mm and the higher burnishing force i.e. 200 N. Indeed, these two parameters increase the magnitude of burnishing pressure and imply an increase in the amount of plastic deformation. A high value of compressive residual stress was obtained with a low feed rate (0.05 mm/rev) and a low cutting speed (100 m/min). This is due to the fact that the metal flow is more regular and greater under these parameters.

X-Ray diffraction with electro polishing was used to evaluate the residual stresses on and below the surface of workpiece along feed and burnishing directions (Figs. 14 and 15). As shown, a distribution of compressive residual stresses is observed on surface and close to surface along the feed and the burnishing directions. These measurements were conducted once the CoTuB process is carried out for various diameters of ball. This phenomenon is due to the *near pasty state* of the superficial layer, which was the result of burnishing force effects applied on the cut surface where the induced thermal softening effect is occurring. As a result, the magnitudes of compressive residual stresses on surface and below along the two directions were highly increased.

The measurement of residual stresses along the feed and the burnishing directions can reach 0.85 mm beneath surface. Figs. 14 and 15 show that CoTuB process produces a compressive layer with a thickness of 0.85 mm in case of ball-burnishing diameter size of 12 mm (σ_{yy} = -640 MPa, σ_{xx} = -320 MPa). The magnitude of compressive residual stresses for other sizes of ball diameter is slightly higher compared to the value obtained by the diameter of 12 mm. In the case of a ball diameter ϕ_B = 10 mm, (σ_{yy} = -740 MPa, σ_{xx} = -388 MPa) and in case of ϕ_B = 8 mm (σ_{yy} = -698 MPa, σ_{xx} = -441 MPa). However, this compressive layer vanishes at a shorter depth which is 0.4 mm for ϕ_B = 10 mm and 0.2 mm for ϕ_B = 10 mm.

In addition, results show that stresses are dependent on the burnishing pressure in the external surface case, which is in good agreement with Hertz's law. According to Figs. 14 and 15, it can be noted that the optimal profile is obtained after a CoTuB operation with a 12 mm ball diameter. In this case, compressive residual stress reached a depth more than 0.8 mm. In fact, the high recovery rate justified this performance, which is induced by the increase of the pass numbers with a high ball diameter and a low feed rate. A schematic representation of this phenomenon is illustrated in Fig. 16.

In the CoTuB profile obtained with a ball diameter of 8 mm, a peak of tensile close to the surface (15 µm from the surface) appeared. Its origin is mainly the high magnitude pressure applied by the ball, which provoked a shearing phenomenon leading to a micro-crack. Potentially, this can imply a risk of cracks which are harmful regarding the workpiece service.

4.2.3 Effects of controllable parameters on micro-hardness

Fig. 17 illustrates the effect of CoTuB parameters on the external surface micro-hardness. It can be observed that the ball burnishing

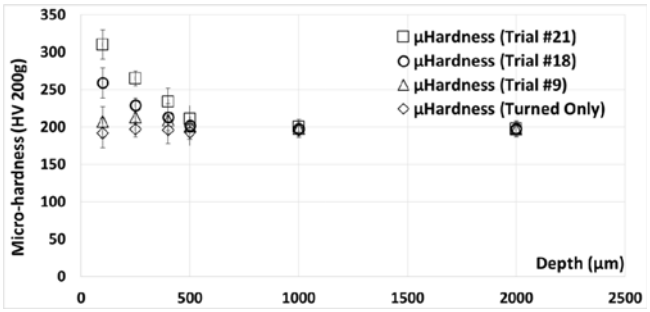

Fig. 18 Evolution of the micro hardness versus the depth

diameter had a major influence on the surface micro-hardness due to the high pressure applied when a small diameter of ball burnishing was used (i.e. referring to Hertz's law). Moreover, according to Hertz's law, the surface micro-hardness increased for burnishing force ranging from 150-200 N. This can be explained by the growth of the burnishing pressure, thus producing a rise in the temperature work surface. Consequently, the increase of work hardening and surface deformation resulted in an increment of surface micro-hardness.

On the other hand, the surface micro-hardness was found to be improved with high cutting speed i.e. 150 m/min and a value of depth of cut equal to 0.1 mm. The surface micro-hardness increased for a feed rate range of 0.05 to 0.1 mm/rev, which is probably related to the rise of the hardening work. During CoTuB experiments, the micro-hardness varied from 208-423 HV and before the CoTuB operation it was 180 HV. Obviously, surface and subsurface of workpiece became harder because of work hardening due to the thermal and the mechanical loads.

In order to identify the alteration in the subsurface micro-structure, both surface and subsurface micro-hardness were measured. Fig. 18 illustrates the variation of micro-hardness with the depth, selected for different CoTuB conditions. The plots presented in Fig. 18 show a significant variation in hardness in the external surface. The high magnitude of hardness is recorded with the small ball diameters referring to Hertz's law and it is caused mainly by the generation of the plastic deformation.

Fig. 18 also shows that hardness increases with an increase in the burnishing pressure values. This performance can be explained by the fact that the pressure exceeds the elastic yield point of the AISI 4140 steel (σ_y = 550 MPa), implying a highly plastic deformation of the superficial layer.

4.2.4 Effects of controllable parameters on micro-structure

For a fundamental understanding, a metallographic examination of combined turning/ball burnishing process has been carried out. The CoTuB process produces a plastic deformation zone that reduces grain sizes along a thin layer of 300 μm from the surface as asserted in Fig. 19. The deformation of the grain on surface is due to the cold-work process during the CoTuB operation.

In order to identify more clearly the influence of process conditions on the subsurface microstructure, a Scanning Electron Microscope (SEM) was employed. Fig. 20 illustrates the obtained micrographs of subsurface micro-structure generated during a CoTuB process. All SEM micrographs show a localized inelastic strain layer in the external

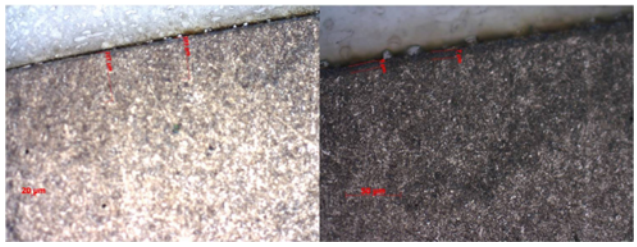

Fig. 19 Optical micrograph of AISI 4140 showing the depth of burnishing

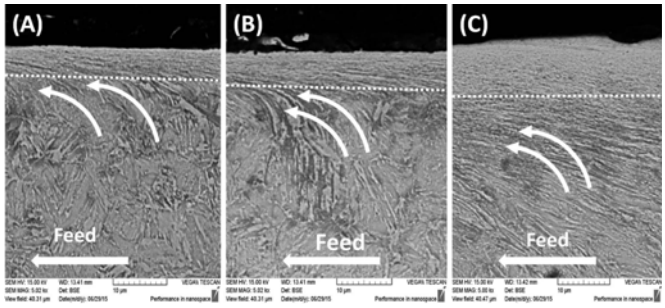

Fig. 20 SEM Micrograph of the layer underneath the CoTuB process (A) ϕ_B = 12 mm (Trial #9); (B) ϕ_B = 10 mm (Trial #18); and (C) ϕ_B = 8 mm (Trial #21)

surface of about 7 to 8 μm. This layer dimension is mostly influenced by the cutting speed and burnishing pressure. Fig. 20 also illustrates that the grain boundaries tend to be deformed in the direction of feed rate due to the high temperature caused by cutting speed and the normal force applied by the ball during the process. Region above the line indicates that the original grains are no longer discernible. Clearly, the above observations demonstrate that high plastic deformation was generated once the CoTuB process is adopted.

4.3 Regression equations

Further investigation was carried out in order to develop polynomial regression models representing the functional relationships between the CoTuB parameters and the performance measures. The surface roughness R_a, the residual stress in the feed direction, the residual stress in the burnishing direction, and the micro-hardness are governed by Eqs. (5), (6), (7), and (8), respectively.

$$\begin{aligned} Ra\ (\mu\text{m}) = &-8.75+0.610\phi_B+0.00092F_B+0.0767V_C \\ &-3.38a_P-9.3f+0.00542\phi_B\cdot V_C-0.91\phi_B\cdot f \\ &+0.00350F_B\cdot a_P-0.0279V_C\cdot a_P \end{aligned} \tag{5}$$

$$\begin{aligned} \sigma_{yy}(\text{MPa}) = &\ 7502-561\phi_B-8.15F_B-39.3V_C-1335a_P \\ &+4284f+4.16\phi_B\cdot V_C-432\phi_B\cdot f+6.64F_B\cdot a_P-0.05V_C\cdot a_P \end{aligned} \tag{6}$$

$$\begin{aligned} \sigma_{xx}(\text{MPa}) = &\ 5418-460\phi_B-5.78F_B-32.09V_C-402a_P \\ &+2937f+3.717\phi_B\cdot V_C-352\phi_B\cdot f+4.607F_B\cdot a_P-4.47V_C\cdot a_P \end{aligned} \tag{7}$$

$$\begin{aligned} \mu H(\text{HV}) = &\ 379-23.1\phi_B-0.603F_B-1.39V_C+67a_P \\ &+1029f+0.047\phi_B\cdot V_C-100\phi_B\cdot f+0.767F_B\cdot a_P-1.37V_C\cdot a_P \end{aligned} \tag{8}$$

Comparisons of the predicted arithmetic values with the measured

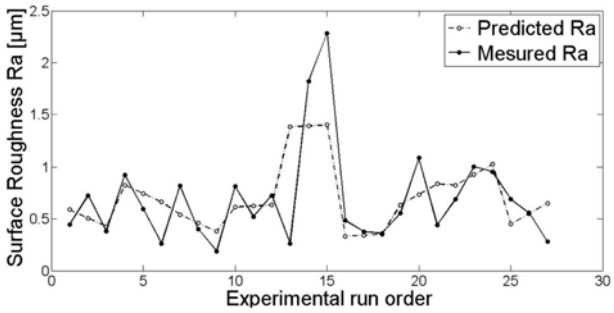

Fig. 21 Comparison between measured and predicted value of surface roughness

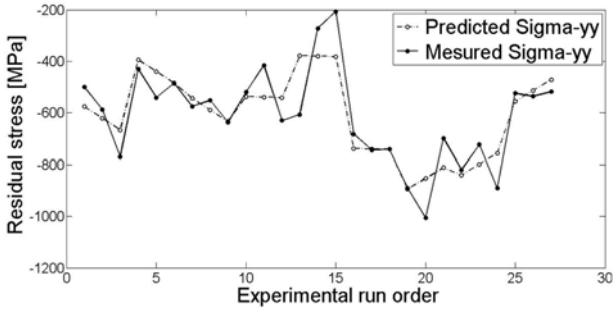

Fig. 22 Comparison between measured and predicted value of residual stress in the feed direction

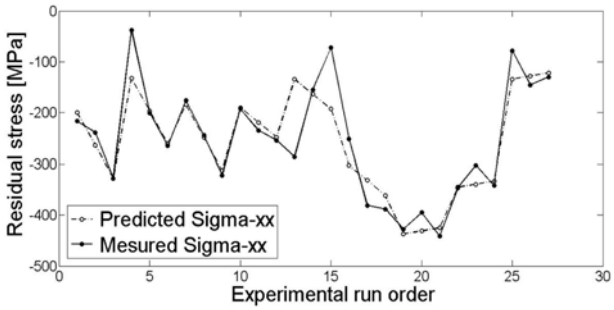

Fig. 23 Comparison between measured and predicted value of residual stress in the burnishing direction

values of surface roughness R_a, the residual stress in the feed direction, the residual stress in the burnishing direction, and the micro-hardness are illustrated in Figs. 21, 22, 23 and 24, respectively. As shown for all parameters, the predicted arithmetic values are generally in good agreement with the measured values.

5. Conclusions

Based on the experimental results on the innovative capabilities of the combined turning-burnishing (CoTuB) process, the following conclusions can be drawn:

1. A new device has been designed and fabricated to carry out CoTuB operation.

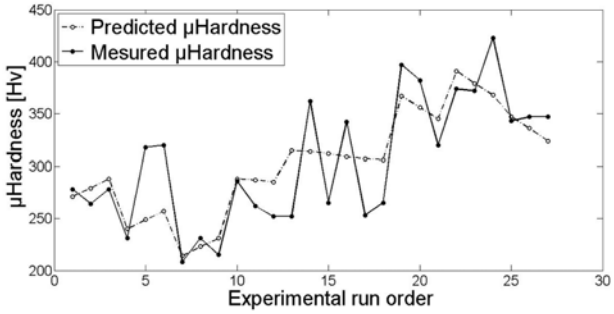

Fig. 24 Comparison between measured and predicted value of micro hardness

2. For the case of AISI 4140 steel, the CoTuB process improves surface roughness about 70% (0.81 μm pre-machined surface can be finished and mechanically treated down to 0.189 μm). The variation of the normal burnishing force has no significant effect on the finished roughness Ra.
3. A feed rate of 0.05 mm/rev gives the best result of surface integrity during the present experimentation at different ball diameters, values of burnishing force, cutting speed and depth of cut,
4. Compressive residual stresses can reach a depth over 0.8 mm with a 12 mm ball diameter and a lower feed rate.
5. Large ball diameter makes residual stress more compressive at the surface with more penetration depth beneath the surface.
6. Ball diameter size and feed rate are closely in relationship with the recovery rate.
7. Hardness increases with a higher burnishing pressure values.
8. CoTuB process improves the surface and subsurface properties in terms of compressive residual stresses and micro-hardness. These properties provide resistance corrosion and wear improvement of workpiece, so enhancing fatigue life.
9. Regression polynomial models were developed for surface performances and can be used as predictive tools.
10. For optimal surface performances when treating AISI 4140 steel, the optimal setting of CoTuB process are: ball diameter (12 mm), burnishing force (100 N), cutting speed (100 m/min), depth of cut (0.5 mm) and feed rate (0.05 mm/rev).
11. Using this process, it is possible to obtain a finished and a treated surface at the same time, from rough conditions.
12. The combined turning and ball-burnishing process improve the production capabilities due to the combination effect.

REFERENCES

1. Hassan, A. M. and Al-Bsharat, A. S., "Improvements in Some Properties of Non-Ferrous Metals by the Application of the Ball-Burnishing Process," Journal of Materials Processing Technology, Vol. 59, No. 3, pp. 250-256, 1996.
2. Murthy, R. and Kotiveerachari, B., "Burnishing of Metallic Surfaces - A Review," Precision Engineering, Vol. 3, No. 3, pp. 172-179, 1981.

3. Hassan, A. M., "The Effects of Ball-and Roller-Burnishing on the Surface Roughness and Hardness of Some Non-Ferrous Metals," Journal of Materials Processing Technology, Vol. 72, No. 3, pp. 385-391, 1997.

4. Rajasekariah, R. and Vaidyanathan, S., "Increasing the Wear-Resistance of Steel Components by Ball Burnishing," Wear, Vol. 34, No. 2, pp. 183-188, 1975.

5. Yao, C., Ma, L., Du, Y., Ren, J., and Zhang, D., "Surface Integrity and Fatigue Behavior in Shot-Peening for High-Speed Milled 7055 Aluminum Alloy," Proceedings of the Institution of Mechanical Engineers, Part B: Journal of Engineering Manufacture, Vol. 231, No. 2, pp. 243-256, 2017.

6. Chomienne, V., "Etude de L'influence de L'intégrit de Surface en Tournage de L'acier 15-5ph sur la Tenue en Fatigue en Flexion Rotative," INSA de Lyon, 2014.

7. Devillez, A., Le Coz, G., Dominiak, S., and Dudzinski, D., "Dry Machining of Inconel 718, Workpiece Surface Integrity," Journal of Materials Processing Technology, Vol. 211, No. 10, pp. 1590-1598, 2011.

8. Mezlini, S., Mzali, S., Sghaier, S., Braham, C., and Kapsa, P., "Effect of a Combined Machining/Burnishing Tool on the Roughness and Mechanical Properties," Lubrication Science, Vol. 26, No. 3, pp. 175-187, 2014.

9. Shirsat, U. and Ahuja, B., "Parametric Analysis of Combined Turning and Ball Burnishing Process," Indian Journal of Engineering and Materials Sciences, Vol. 11, No. 5, pp. 391-396, 2004.

10. Axinte, D. A. and Gindy, N., "Turning Assisted with Deep Cold Rolling - A Cost Efficient Hybrid Process for Workpiece Surface Quality Enhancement," Proceedings of the Institution of Mechanical Engineers, Part B: Journal of Engineering Manufacture, Vol. 218, No. 7, pp. 807-811, 2004.

11. Laouar, L., Hamadache, H., Saad, S., Bouchelaghem, A., and Mekhilef, S., "Mechanical Surface Treatment of Steel-Optimization Parameters of Regime," Physics Procedia, Vol. 2, No. 3, pp. 1213-1221, 2009.

12. Aouici, H., Yallese, M. A., Chaoui, K., Mabrouki, T., and Rigal, J.-F., "Analysis of Surface Roughness and Cutting Force Components in Hard Turning with CBN Tool: Prediction Model and Cutting Conditions Optimization," Measurement, Vol. 45, No. 3, pp. 344-353, 2012.

13. Cohen, G., "Etude des effets thermiques et mécaniques en usinage à sec. Application à la qualité de la pièce en tournage," Ph.D. Thesis, Université Paul Sabatier, 2009.

14. Sai, W. B., Salah, N. B., and Lebrun, J., "Influence of Machining by Finishing Milling on Surface Characteristics," International Journal of Machine Tools and Manufacture, Vol. 41, No. 3, pp. 443-450, 2001.

15. Jaffery, S. H. I., Khan, M., Ali, L., and Mativenga, P. T., "Statistical Analysis of Process Parameters in Micromachining of Ti-6Al-4V Alloy," Proceedings of the Institution of Mechanical Engineers, Part B: Journal of Engineering Manufacture, Vol. 230, No. 6, pp. 1017-1034, 2016.

16. Chen, L., El-Wardany, T., and Harris, W., "Modelling the Effects of Flank Wear Land and Chip Formation on Residual Stresses," CIRP Annals-Manufacturing Technology, Vol. 53, No. 1, pp. 95-98, 2004.

17. Avilés, R., Albizuri, J., Rodríguez, A., and de Lacalle, L. L., "Influence of Low-Plasticity Ball Burnishing on the High-Cycle Fatigue Strength of Medium Carbon AISI 1045 Steel," International Journal of Fatigue, Vol. 55, pp. 230-244, 2013.

18. Revankar, G. D., Shetty, R., Rao, S. S., and Gaitonde, V. N., "Analysis of Surface Roughness and Hardness in Ball Burnishing of Titanium Alloy," Measurement, Vol. 58, pp. 256-268, 2014.

19. Gharbi, F., Sghaier, S., Hamdi, H., and Benameur, T., "Ductility Improvement of Aluminum 1050A Rolled Sheet by a Newly Designed Ball Burnishing Tool Device," The International Journal of Advanced Manufacturing Technology, Vol. 60, No. 1, pp. 87-99, 2012.

20. Rodríguez, A., de Lacalle, L. L., Celaya, A., Lamikiz, A., and Albizuri, J., "Surface Improvement of Shafts by the Deep Ball-Burnishing Technique," Surface and Coatings Technology, Vol. 206, No. 11, pp. 2817-2824, 2012.

21. de Lacalle, L. L., Lamikiz, A., Munoa, J., and Sánchez, J., "Quality Improvement of Ball-End Milled Sculptured Surfaces by Ball Burnishing," International Journal of Machine Tools and Manufacture, Vol. 45, No. 15, pp. 1659-1668, 2005.

22. Gharbi, F., Sghaier, S., Morel, F., and Benameur, T., "Experimental Investigation of the Effect of Burnishing Force on Service Properties of AISI 1010 Steel Plates," Journal of Materials Engineering and Performance, Vol. 24, No. 2, pp. 721-725, 2015.

23. Gharbi, F., Sghaier, S., Al-Fadhalah, K., and Benameur, T., "Effect of Ball Burnishing Process on the Surface Quality and Microstructure Properties of AISI 1010 Steel Plates," Journal of Materials Engineering and Performance, Vol. 20, No. 6, pp. 903-910, 2011.

24. El-Taweel, T. and El-Axir, M., "Analysis and Optimization of The Ball Burnishing Process through the Taguchi Technique," The International Journal of Advanced Manufacturing Technology, Vol. 41, No. 3, pp. 301-310, 2009.

25. Javidi, A., Rieger, U., and Eichlseder, W., "The Effect of Machining on the Surface Integrity and Fatigue Life," International Journal of Fatigue, Vol. 30, No. 10, pp. 2050-2055, 2008.

26. Sasahara, H., "The Effect on Fatigue Life of Residual Stress and Surface Hardness Resulting from Different Cutting Conditions of 0.45% C Steel," International Journal of Machine Tools and Manufacture, Vol. 45, No. 2, pp. 131-136, 2005.

27. Hamadache, H., Laouar, L., Zeghib, N., and Chaoui, K., "Characteristics of Rb40 Steel Superficial Layer under Ball and Roller Burnishing," Journal of Materials Processing Technology, Vol. 180, No. 1, pp. 130-136, 2006.

28. Hassan, A. M. and Al-Dhifi, S. Z., "Improvement in the Wear Resistance of Brass Components by the Ball Burnishing Process," Journal of Materials Processing Technology, Vol. 96, No. 1, pp. 73-80, 1999.

29. Jinlong, L. and Hongyun, L., "Effect of Surface Burnishing on Texture and Corrosion Behavior of 2024 Aluminum Alloy," Surface and Coatings Technology, Vol. 235, pp. 513-520, 2013.